UPSCALING SOIL MOISTURE MEASUREMENTS FROM IN SITU SENSORS

By

WILLIAM GERALD BROWN JR

Bachelor of Science in Environmental Science

Oklahoma State University

Stillwater, Oklahoma

2019

Submitted to the Faculty of the
Graduate College of the
Oklahoma State University
in partial fulfillment of
the requirements for
the Degree of
MASTER OF SCIENCE
July 2021

`

UPSCALING SOIL MOISTURE MEASUREMENTS

FROM IN SITU SENSORS

Thesis Approved:

Dr. Tyson Ochsner (Thesis Advisor)

Dr. Sergio Abit

Dr. Chris Zou

`

ACKNOWLEDGEMENTS

Dr. Ochsner, I cannot express how much you have helped me both personally and professionally. Thank you for your patience and knowledge of soil physics that you so freely give away to any and all.

I would like to thank Dr. Michael Cosh for providing funding for this research.

I would like to thank my committee members, Dr. Chris Zou and Dr. Sergio Abit for their suggestions and comments on improving this thesis.

For all the help with my research and making me feel welcome in the group, I want to thank Dr. Jingnuo Dong and Dr. Briana Wyatt.

I would like to thank my parents for being with me throughout my educational endeavors. Without their help, it would not have been possible.

`

Name: WILLIAM GERALD BROWN JR

Date of Degree: July 2021

Title of Study: UPSCALING SOIL MOISTURE MEASUREMENTS FROM IN SITU SENSORS

Major Field: PLANT AND SOIL SCIENCES

Abstract:

Accurate, field-scale soil moisture information is needed to match the spatial scale of land and water management decisions related to agricultural production and environmental protection. Soil moisture measurements at the field-scale are limited because the resolution of most satellite-based soil moisture products is too coarse, while most in situ monitoring networks can provide only point-scale, not field-scale, data. This research attempts to develop a broadly applicable upscaling approach for observations from in situ soil moisture sensors using data from the Marena, Oklahoma, In Situ Sensor Testbed (MOISST) and a cosmic-ray neutron rover. The landscape at the MOISST site is predominantly grassland with some deciduous trees and eastern redcedar intermixed. Cosmic-ray neutron rover survey data were used to measure average soil moisture for the ~64 ha site on 12 dates in 2019-2020. The relationships between the point-scale in situ data and the field-scale rover data were examined using data from six in situ stations. Statistical modeling was used to identify the soil, terrain, and vegetation properties that influence these relationships. Site-specific linear upscaling models estimated the field average soil moisture with root mean squared error (RMSE) values ranging from 0.014 – 0.022 cm^3 cm^{-3}, but these models are not transferable to other sites. A general upscaling model using soil texture data was developed and achieved RMSE values ranging from 0.017 – 0.038 cm^3 cm^{-3} for four calibration sites and values ranging from 0.015 – 0.021 cm^3 cm^{-3} for two validation sites. The general upscaling model demonstrated accuracy better than the commonly used threshold of 0.04 cm^3 cm^{-3} and should be further tested to evaluate its suitability as a broadly applicable upscaling approach for point-scale in situ monitoring stations.

`

TABLE OF CONTENTS

Chapter Page

I. INTRODUCTION 1

II. MATERIALS AND METHODS 5

III. RESULTS 15

IV. DISCUSSION 19

V. CONCLUSION 21

REFERENCES 22

APPENDICES 38

`

LIST OF TABLES

Table Page

1 Statistical comparison of field-scale average volumetric water content versus point-scale measurements at four calibration sites and two validation sites in the Marena, Oklahoma, In Situ Sensor Testbed (MOISST) without upscaling, after application of site-specific linear upscaling relationships, and after application of a general upscaling model. Statistical indicators include the Nash-Sutcliffe Efficiency (NSE), root mean squared error (RMSE), bias, regression slope, and regression intercept.…….....28

2 Depth-weighted sand content and clay content measured at four sites used to calibrate the general upscaling model and two sites used to validate the model. Also listed are elevation for each site determined using LIDAR data with 2-m resolution and average NDVI for the study period using 30-m resolution data from Landsat 8. The depth-weighted field average sand content and clay content from the POLARIS data set and field average elevation and NDVI are also listed. 29

A1 Soil physical properties for sites A, B, C, and D.....41

A2 Soil physical properties for validation sites, JFSP Site 5 and 6 42

`

LIST OF FIGURES

Figure Page

Figure 1 Map of Marena, Oklahoma In Situ Sensor Testbed (MOISST), located southwest of Stillwater, OK. Yellow letters designate sensor testbeds (A-D), and the upper right quadrant shows the Oklahoma Mesonet site (MARE).....30

Figure 2 Depth-weighted volumetric water content data from four in situ monitoring sites during the period of the study. Black circles are field-scale averages measured using the rover on each survey date 31

Figure 3 Map displaying kriged soil volumetric water content estimates derived from the rover data on 16 Sep. 2020, averaging 0.302 cm^3 cm^{-3}. Black dots represent the locations of rover measurements. Coordinates are UTM, Zone 14.....32

Figure 4 Map displaying kriged soil volumetric water content estimates derived from the rover data on 30 Sep. 2020, averaging 0.195 cm^3 cm^{-3}. Black dots represent the locations of rover measurements. Coordinates are UTM, Zone 14.....33

Figure 5 Comparison of field-scale volumetric water content estimate from the cosmic-ray neutron rover surveys vs. depth-weighted point-scale

volumetric water content measurements from the in situ sensors at four sites for the twelve survey dates. Days with missing point-scale data were omitted 34

Figure 6 Depth-weighted sand content (top) and depth-weighted clay content (bottom) for the study site based on 30 m resolution POLARIS data. Coordinates are UTM, Zone 14.....35

Figure 7 Map of elevation at the study site based on 2 m horizontal resolution LIDAR data from USGS. Coordinates are UTM, Zone 14.....36

Figure 8 NDVI averaged over the period of Nov. 2019 – Oct. 2020 based on 30 m resolution Landsat 8 data. Coordinates are UTM, Zone 14. 37

Figure 9 LASSO regression results showing number of predictor variables used and estimated RMSE. The most influential predictor variables were: (1) point-scale volumetric water content, (2) sand content, and (3) NDVI 38

Figure 10 Upscaled soil volumetric water content estimates from each of the four calibration sites after applying the general upscaling model compared with the field-scale water content measurements from the cosmic-ray neutron rover. 39

Figure 11 Point-scale soil volumetric water content measurements from each of the two validation sites and upscaled water content estimates for those sites after applying the general upscaling model compared with the

`

field-scale water content measurements from the cosmic-ray neutron rover.....40

`

CHAPTER I

INTRODUCTION

Accurate soil moisture measurements at the field-scale (~10 – 100 ha) are needed to match the typical spatial scale of land and water management decisions (Robinson et al., 2008). Soil moisture is variable both spatially and temporally, and better methods for estimating soil moisture at the field scale are needed for better prediction of moisture dependent processes (Western et al., 2002). Direct soil moisture measurements at the field-scale are limited because the resolution of most satellite-based soil moisture products is too coarse, while most in situ monitoring networks can provide only point-scale, not field-scale data. High resolution soil moisture maps can be generated using data from in situ monitoring networks in conjunction with digital soil data and gridded precipitation data (Ochsner et al., 2019), but the uncertainty of the resulting maps is likely to be inflated if the point-scale observations are not appropriately upscaled to match the map resolution. In this context, when point-scale measurements are mathematically transferred in an attempt to make them better represent the average conditions across a larger geographic area, this process is called upscaling.

Upscaling methods for point-scale measurements include temporal stability approaches which identify individual point-scale sensors from a network of sensors that display a consistent relationship to the network average over time. One type of temporal stability analysis is the mean relative difference method, which compares the average of a network to a particular sensor and

`

shows if the sensor is consistently higher or lower than the average. Applying the mean relative difference method to measurements from the 610-km^2 Little Washita River Watershed Micronet in Oklahoma showed that four of the thirteen monitoring locations were temporally stable and estimated the network average with a root mean squared error < 0.04 cm^3 cm^{-3} (Cosh et al., 2006).

A smaller study in Maryland applied the mean relative difference method to a temporally stable in situ sensor installed in a 21 ha corn field and achieved an (Nash-Sutcliffe Efficiency) NSE of 0.82 in estimating the network average (De Lannoy et al., 2007). These studies show good accuracy and precision but also highlight drawbacks such as having sensors installed in a representative region of interest with time-stable characteristics (Loew and Schlenz, 2011) as well as specificity of the model to the site.

A more sophisticated method for upscaling soil moisture data from an in situ network is Random Forests regression. This machine learning method uses multiple geophysical data layers and measurements from in situ sensors to produce 100-m gridded estimates of soil moisture (Clewley et al., 2017). Upscaled soil moisture estimates for the network or domain are produced by simply averaging the gridded estimates. In their study to validate satellite soil moisture sensing products, applied this method achieving a root mean square error (RMSE) of 0.025 cm^3 cm^{-3} at the SMAPVEX12 site in Winnipeg, Canada. Using the random forest regression on four sites in the United States and Canada, Whitcomb et al. (2020) achieved RMSE results ranging from 0.015 – 0.037 cm^3 cm^{-3}. The random forests regression approach demonstrates acceptable accuracy (RMSE <0.04 cm^3 cm^{-3}) and makes beneficial use of available supporting data such as topography, land cover, and soil texture, but the resulting models are site specific and require extensive training data for each site.

`

In order to develop upscaling methods that are more broadly applicable to the stations in sparse in situ networks and to single monitoring sites within a field, accurate measurements of soil moisture at the field scale are required. One promising approach for measuring soil moisture at the field-scale is by cosmic-ray neutron detection (Dong et al., 2014). Cosmic rays are high energy sub-atomic particles (mostly protons) (Zreda et al., 2008) originating in outer space, which interact with atmospheric nuclei to create fast neutrons (Hess et al., 1959; Zreda et al., 2012). These fast moving neutrons may collide with other atmosphere nuclei creating more fast neutrons, which continue toward the Earth's surface and can also react with nuclei in the top 1 m of soils producing additional fast neutrons (Desilets et al., 2010). Neutrons and hydrogen atoms have similar masses and upon impact tend to have elastic collisions, in which the neutrons experience kinetic energy loss. Through repeated collisions the fast neutrons can eventually become slow or thermal neutrons. As this happens, the intensity of the fast neutrons reaches a quasi-steady state in the atmosphere 1 - 2 m above the soil. The moderating effect of hydrogen on these neutrons gives rise to an inverse correlation of fast neutron intensity with soil moisture in the surrounding landscape. The cosmic-ray neutron rover is a portable device that measures the fast neutron intensity near the land surface and can be used to generate accurate field-scale soil moisture estimates (Dong et al., 2014).

The objective of this research is to develop a broadly applicable upscaling approach for point-scale in situ soil moisture sensors using data from a cosmic-ray neutron rover. Survey data from the rover were used to produce field-scale soil moisture values, and relationships between the point-scale in situ data and the field-scale rover data were determined for each of four in situ stations. Statistical modeling was used to identify the soil, vegetation, and terrain properties that

`

influence these relationships and hold promise for enabling broadly applicable upscaling approaches for other locations that lack field-scale data.

`

CHAPTER II

MATERIALS AND METHODS

Site Description

This study was conducted at the Marena, Oklahoma, In Situ Sensor Testbed (MOISST) site located on the Oklahoma State University (OSU) Range Research Station ~13 km southwest of Stillwater, Oklahoma. The MOISST site was established in 2010 to facilitate inter-comparisons of different soil moisture sensing technologies in support of NASA's Soil Moisture Active Passive (SMAP) mission (Cosh et al., 2016). The vegetation at the site is predominantly native grasses with some scattered stands of post-oak (*Quercus stellata*) and eastern redcedar (*Juniperus virginiana L.*) trees (Figure 1). This site is under patch burn management (Sharma et al., 2021) and is grazed by cattle and goats at a moderate stocking rate. As of 2016, using the previous 15 years of data, annual precipitation averaged 876 mm with an annual average temperature of 15.6°C (Cosh et al., 2016). Total rainfall during the 12-month study period (Nov. 2019 – Dec. 2020) was 882 mm collected from Oklahoma Mesonet Marena (MARE) station located at the site (McPherson et al., 2007). Coyle-Lucien and Grainola-Lucien complexes make up the two dominant soil map units within the test site. The Coyle series (siliceous, active, thermic Udic Argiustolls) are fine loamy, moderately deep, well-drained soils weathered from sandstone. The Grainola series (fine, mixed active, thermic Udertic Haplustalfs) are moderately deep, well drained soils weathered from shale. The Lucien series (loamy, mixed, superactive,

`

thermic, shallow Udic Haplustolls) are very fine sandy loam, shallow, well drained soils weathered from sandstone.

In Situ Sensors

There are four primary (calibration) sites within the testbed at which in situ sensors are installed (Sites A, B, C, and D, Figure 1). Site A is located at 36.06351° N, -97.21697° W. From that point, site C is located ~50 m west, site B is located ~100 m south, and site D is located ~200 m northeast (Figure 1). Additionally, located within the study site, are two validation sites (Sites 5 and 6 [6 not shown], Figure 1). Soil water content reflectometers (CS-655, Campbell Scientific, Logan, Utah) were installed horizontally at 5, 10, 20, and 50-cm depths, except at site C where the deepest sensor was at 30 cm instead of 50 cm due to shallow bedrock. The sensors have two stainless steel rods spaced 32 mm apart and 120 mm long that form an open-ended transmission line. An oscillating signal is applied to the rods, and dielectric permittivity is estimated according to the travel time of the signal. Permittivity (K_a) is then used to calculate volumetric water content (VWC) by:

$$\theta_v = C_0 + C_1 K_a + C_2 K_a^2 + C_3 K_a^3 \qquad (1)$$

where $C_{0\,=}$ = -0.53, C_1 = 0.0292, and C_3 = 0.0000043 (Topp et al., 1980). Measurements were taken each minute, and at the top of each hour the last five measurements were averaged for an hourly average and recorded on a data logger (CR-1000,Campbell Scientific, Logan, Utah). The data from the in situ sensors were depth-weighted using the approach of Kohli et al., (2015)

`

assuming a horizontal distance from the rover of 200 m, corresponding approximately to the radius of the rover footprint.

Rover Description and Calibration

The custom built cosmic-ray neutron rover (Hydroinnova, LLC) consisted of two instrument enclosures that each held two ^{3}He-filled proportional neutron counters encased in 2.5-cm thick high-density polyethylene (Dong and Ochsner, 2018). Connected to the counters are neutron pulse modules (Q-NPM_3000, Questa Instruments, LLC) that total the neutron counts for 60-s intervals and send them, via environmentally sealed ethernet cable with bulging locking connectors, to a separate case with an integrated data logger (Q-DL_2100, Questa Instruments, LLC) with a barometric pressure sensor, GPS receiver, and a removable SD card. Air temperature and relative humidity were measured using an external sensor (CS-215, Campbell Scientific, Logan, Utah) mounted at 2-m height.

The calibration data for the rover were taken from a previous study using the same instrument (Dong and Ochsner, 2018). Transforming raw neutron counts to volumetric water content required accounting for varying atmospheric conditions that affect neutron intensity at ground-level. Measurements of barometric pressure, relative humidity, and air temperature were used to normalize the neutron counts. A reference pressure of 965 mb and mass attenuation length of 130 mbar (Dong and Ochsner, 2018), were used to correct for atmospheric pressure variation [Eq. 1; Andreasen et al. (2017)]. A reference water vapor concentration of 0 g m^{-3} was used in the normalization of the neutron counts [Eq. 3; Andreasen et al. (2017)]. Relative humidity and air temperature measurements from the rover surveys were used to calculate the atmospheric water vapor concentration (Rosolem et al., 2013). Incoming neutron flux varies both

`

spatially and temporally. Data obtained from the Dourbes station (Dong and Ochsner, 2018) of the neutron monitor database (http://www.nmdb.eu/) were used for the incoming flux correction [Eq. 2; Andreasen et al. (2017)]. The pressure, water vapor, and incoming neutron flux corrections were then used to convert the measured neutron counts to corrected neutron counts [Eq. 4; Andreasen et al. (2017)]. Corrected neutron counts were converted to soil volumetric water content using:

$$\theta_v = \left(\frac{a_0}{\left({}^{N_{cor}}/_{N_0} \right) - a_1} - a_2 - W_{lat} \right) * \frac{\rho_b}{\rho_w} \qquad (2)$$

where θ_v ($cm^3\ cm^{-3}$) is soil volumetric water content, W_{lat} is the soil lattice water content ($g\ g^{-1}$), N_{cor} are the corrected neutron counts, and $a_0 = 0.808$, $a_1 = 0.372$, and $a_2 = 0.115$ are constants (Desilets et al., 2010). N_0 represents the neutron counts per minute over dry soil using the reference conditions defined above. N_0 was calculated using previous simultaneous soil sampling and rover data collected at four Oklahoma Mesonet sites (Lahoma, Marena, Marshall and Perkins) (Dong and Ochsner, 2018). For each site, N_0 was estimated by solving Eq. (2) for N_0 with θ_v and ρ_b determined by soil sampling. The depth weighting function of Köhli et al. (2015) was applied to individual soil samples within the rover footprint when calculating θ_v for Eq. (2). The horizontal weighting function of Köhli et al. (2015) was applied when calculating both θ_v and ρ_b for Eq. (2). The average N_0 value across the four sites was 596 ±6 cpm, and this value was used for subsequent θ_v estimates using Eq. (2). A lattice water content value of 0.032 $g\ g^{-1}$ was used for the MOISST site in Eq. (2) based on the average measured lattice water content from 13 samples. The field averaged bulk density for the MOISST site was 1.35 $g\ cm^{-3}$.

`

After calibrating the neutron counts, measurements with identical locations were removed. Once the corrected counts were converted to volumetric water content, any estimates < 0 cm^3 cm^{-3} or > 0.5 cm^3 cm^{-3} were discarded.

Rover Surveys

The area traversed during the rover surveys measured ~800 m x 800 m and was divided into 200-m sections for data collection. Data were collected on 15 Nov. 2019; 15 Feb. 2020; 10, 17, and 24 June 2020; 8 and 15 July 2020; 10, and 26 Aug. 2020; 16 and 30 Sep. 2020; and 16 Oct. 2020.

A utility terrain vehicle (Kawasaki Mule) was used to transport the rover over the test area to collect neutron counts. In order to achieve an evenly spaced and thorough dataset, the test area was divided into 200-m segments corresponding to the rover's footprint of ~400-m diameter (Köhli et al., 2015). Two serpentine passes were made during the course of a survey to facilitate gathering an adequate number of neutron counts for precise soil moisture estimation. The duration of the surveys ranged from 79 to 228 minutes with an average of 129 minutes. This equates to an average driving speed of 5.6 km h^{-1} over the 12 survey dates. It was not possible to traverse two points on the east-west paths located in the southeast quadrant of the site due to a small ravine and dense vegetation. At those locations, once the impassable point was reached, the rover path was changed to follow the natural contour of the ravine either north or south until the next east-west path was intersected. The field-scale average soil moisture was calculated by

`

converting each of the one-minute neutron count totals to an estimate of volumetric water content using Eq. (2) and averaging all the water content estimates for each individual survey date.

In order to generate field-scale soil moisture maps for illustrative purposes, empirical semivariograms were created from the rover soil moisture estimates, then fit with both spherical and exponential variogram models. The spherical had the minimum weighted mean squared error and was thus chosen for all twelve survey dates. The prediction grid for mapping soil moisture was constructed in UTM coordinates with 50-m spacing. Ordinary kriging was then used to estimate soil water content at each prediction point on each survey date.

Ancillary Data

Intact soil cores were taken adjacent to each in situ monitoring station to characterize soil physical properties. That characterization included laboratory measurements of the following properties: bulk density; volumetric water content retained at -10, -33, and -1500 kpa; and percent sand, silt, and clay. A 30-m resolution digital soils dataset, POLARIS, was used to estimate the field average sand and clay content of the MOISST site, along with creating maps of sand and clay content (Chaney et al., 2016). The POLARIS dataset, (http://hydrology.cee.duke.edu/POLARIS/PROPERTIES/v1.0/), was created to re-map the Soil Survey Geographic database (SSURGO) by digital soil mapping techniques. POLARIS is based on a high performance computing algorithm that applies environmental covariates, mainly elevation, parent material, and land cover, to fill in the gaps of missing data in the SSURGO database and smooth out the discontinuities (Chaney et al., 2016). The POLARIS data set is not a

`

replacement for SSURGO, but it does provide gridded 30-m resolution soil data across the contiguous US that are harmonized and spatially complete. Both the measured sand and clay contents at the in situ monitoring sites and the POLARIS sand and clay data for the entire field were depth-averaged using the Köhli et al. (2015) depth-weighting scheme.

Elevation data were downloaded from the Geospatial Data Gateway operated by the USDA-NRCS. Elevations were determined using Light Detection and Ranging (LIDAR), a remote sensing technology that measures scattered light to target the range of remote targets. LIDAR has been widely used to produce accurate digital elevation models. The bare earth digital elevation model for the study site with 2-m horizontal resolution was downloaded in Geo-TIFF format and used to determine the elevation of each in situ monitoring station.

Normalized Difference Vegetation Index (NDVI) data were measured by the Landsat 8 satellite that is part of the USGS National Land Imaging (NLI) Program. Orbiting the earth at an altitude of 705 km, Landsat 8 acquires ~740 scenes daily with a footprint of 185 km x 180 km. Landsat 8 data were obtained and processed using a custom script on Google Earth Engine (https://code.earthengine.google.come/b8cc772541083ald20f9ffa8b0585066). The NDVI data have a 30-m resolution and the average NDVI for each pixel in the study area was determined based on all available scenes during the 12-month study period.

Statistical Analysis and Upscaling

`

The extent of agreement between the raw point-scale and field-scale data was first analyzed. The Nash-Sutcliffe Efficiency (NSE) (Ritter and Muñoz-Carpena, 2013) was calculated as:

$$NSE = 1 - \frac{SSE}{SST} \quad (3)$$

where SSE is sum of squared prediction error and SST is the total sum of squares corrected for the mean. The NSE tells how well the predicted values fit the 1:1 line, with 1 meaning the model has perfect predictive power and 0 meaning it has the same predictive ability as using the mean of the dependent variable. The root mean squared error (RMSE) was also calculated using:

$$RMSE = \sqrt{\frac{SSE}{n}} \quad (4)$$

where n is the number of measurement pairs. RMSE is a good indicator of predictive accuracy with values that range from zero (indicating a perfect fit) upwards to infinity. The bias was also calculated by taking the mean of the observed differences between the depth-weighted point-scale and field-scale measurements.

For the site-specific upscaling, linear regression models were fit with the field-scale average soil moisture as measured by the rover as the dependent variable and the point-scale depth-weighted soil moisture from each monitoring station as the independent variable. The resulting models represent “best case” linear upscaling models for these sites, and their performance was summarized by the NSE, RMSE, and the bias. The NSE and RMSE were calculated as above and the bias in this case is the mean of the difference between the observed point-scale measurements and the predicted or upscaled measurements.

`

In order to develop a general upscaling model, four candidate predictor variables were considered, along with their interactions with the point-scale data. The candidate predictors were sand and clay content, NDVI, and elevation and all were calculated as the difference between the measured value at the selected monitoring station and the field mean. For sand and clay contents the lab-measured values at the monitoring stations were used instead of the POLARIS estimates for these locations because the lab measured values have less uncertainty. In order to determine the most influential predictors for use in a parsimonious upscaling model, the candidate predictors were inserted into a Least Absolute Shrinkage and Selection Operator (LASSO) regression model. The LASSO algorithm solves the minimization problem:

$$\frac{min}{\beta_0,\beta}\left(\frac{1}{2N}\sum_{i=1}^{N}\left(y_i-\beta_0-x_i^T\beta\right)^2+\lambda\sum_{j=1}^{p}|\beta_j|\right) \qquad (5)$$

where N is number of observations, y_i is the field-scale soil moisture observation i, x_i is the vector of candidate predictors for observation i, λ is a nonnegative regularization parameter, and β_0 and β are the intercept and coefficients of the upscaling model with P candidate predictors. This algorithm solves the minimization problem repeatedly using a sequence of increasing λ values, which gradually "shrinks" the number of variables with non-zero coefficients. As the goal of this research is to create a general model that can be used for upscaling at other sites, LASSO regression was ideal in helping to identify the most essential predictor variables. The most important predictors identified by LASSO regression were then input into a multiple linear regression model so that the best fit was achieved.

The suitability of the resulting upscaling model was evaluated by an F test comparing the full model with all candidate predictors included and the reduced model containing only the most

`

significant predictors identified by the LASSO regression. The F test evaluates the null hypothesis that the variables excluded have no predictive power, i.e., their true coefficients were zero (Ott and Longnecker, 2000). The F statistic was calculated by:

$$F = \frac{[SS(Regression,\ complete) - SS(Regression,\ reduced)] \div (k-g)}{\frac{SS(Regression,\ complete)}{[n-(k+1)]}} \quad (6)$$

where *SS*(*Regression, complete*) is the regression sum of squares (all variables), *SS*(*Regression, reduced*) is the regression sum of squares (selected variables only), *k* is the total number of variables, *g* is the number of variables selected for the upscaling model, and *n* is the number of measurements. If F is less than the critical F value for $\alpha = 0.05$ and $n - (k + 1)$ degrees of freedom, then we fail to reject the null hypothesis. Matlab R2021a was used to process and analyze all the data.

`

CHAPTER III

RESULTS

A time series of the data from the in situ sensors over the 12-month study period is shown in Figure 2 along with the neutron rover field average values plotted for the survey dates. The point-scale volumetric water content varied over a wide range between 0.07 to 0.47 cm^3 cm^{-3}. The point-scale soil moisture data reflect the soil texture variations, as site C, with the greatest sand content, had the least soil moisture for most dates in the study period. In contrast, Site B has the greatest clay content below the 15-cm depth (Table A1) and had the greatest soil moisture for most dates in the study period. The field-scale average soil moisture as measured by the rover ranged from a maximum of 0.43 cm^3 cm^{-3} on 15 November 2019 to a minimum of 0.15 cm^3 cm^{-3} 17 June 2020.

Field-scale soil moisture maps were created contrasting days with relatively high and low soil moisture contents, 16 September (Figure 3) and 30 September (Figure 4) respectively. Field-scale volumetric water content averaged 0.33 cm^3 cm^{-3} on 16 September and ranged from 0.18 – 0.47 cm^3 cm^{-3}. Field-scale volumetric water content averaged 0.20 cm^3 cm^{-3} on 30 September, with the rover estimates ranging from 0.09 – 0.48 cm^3 cm^{-3}. The range of estimates for both days are actual rover data on the survey date as opposed to the 50-m grid-based rover data. The standard deviation (σ) and coefficient of variation (CV) were 0.1103 cm^3 cm^{-3} and 0.335 on 16 September and 0.065 cm^3 cm^{-3} and 0.333 on 30 September. The water content maps tended to

`

partially reflect the natural topography with the lower elevations having higher soil moisture values and the upper elevations showing lower soil moisture values. However, the uncertainty of volumetric water content estimate at any specific location in the map is relatively large as indicated by the square root of the mean kriging variance, which ranged from 0.0438 to 0.0725 $cm^3\ cm^{-3}$ across the 12 survey dates. In contrast, the rover provided precise estimates of the field-scale average soil moisture as reflected in the standard error of the mean which was < 0.0075 $cm^3\ cm^{-3}$ across all survey dates.

Figure 5 shows the rover field-scale water content average versus the point-scale sensor water content depth-weighted average for the 12 survey days. Overall, the field-scale observations were greater than the point-scale observations for all the calibration sites except site B, which not only has the highest clay content below the 15-cm depth, but also has the highest NSE of 0.963 and lowest RMSE of 0.02 $cm^3\ cm^{-3}$ when compared to the field-scale observations without upscaling (Table 1). Point-scale data from Site C showed the greatest discrepancies from the field-observations, with consistently lower soil moisture values leading to a NSE near 0 and a RMSE = 0.10 $cm^3\ cm^{-3}$ without upscaling. The linearity of the relationship between the point-scale and field-scale soil moisture is clearly evident (Figure 5) and is reflected in the statistics for the site-specific upscaling models (Table 1) which were derived using linear regression. For those models, the NSE values are all > 0.96 and the RMSE values are all ≤ 0.022 $cm^3\ cm^{-3}$.

Candidate predictors for the generalized upscaling model included depth-weighted sand and clay content which are mapped in Figure 6. The sand contents ranged from 17 to 71% and were inversely related to the clay contents which ranged from 9 to 30% based on the POLARIS data. The measured sand and clay contents for the in situ stations (Table 2) highlight the contrast

`

of site C with the other sites, as site C has the greatest sand content and lowest clay content. Elevation (Figure 7) was also included as a candidate predictor, and the topographic map clearly shows the natural valley in the Southeast quadrant of the study site. However, the available in situ stations are all located at the middle to high elevations of the field (Table 2). Average NDVI values over the study period are mapped in Figure 8. Relatively high NDVI values are associated with the trees that line the valley in the southeast, while the grassland dominated areas have lower NDVI values. The in situ stations had NDVI values near the middle of the range (Table 2). As expected, the LASSO regression indicated that point-scale volumetric water content was the most important predictor to include followed by sand content and NDVI data (Figure 9). Although the model produced a RMSE of ~0.024 cm^3 cm^{-3} for the calibration sites using these three parameters, performance at the validation sites was poor (data not shown). We therefore include only point-scale water content and sand content in the general upscaling model. An F test comparing this model with only two predictor variables to the full model with nine predictors resulted in an F value of 0.29. This was less than the critical F value of 2.30, therefore we failed to reject the null hypothesis that the predictors omitted from the smaller model have no predictive power at the 95% confidence level. The general upscaling model is thus:

$$\theta_{us} = b_0 + b_1 * \theta_{ps} + b_2 * \Delta sand \qquad (7)$$

where θ_{us} is the upscaled volumetric water content, θ_{ps} is the depth-weighted in situ point-scale measurement, $b_0 = 0.0593$, $b_1 = 1.0021$, $b_2 = 0.0034$ (coefficients determined by multiple regression) and $\Delta sand$ is the difference between the depth-weighted sand content (%) measured at the in situ monitoring location and the depth-weighted, field-averaged sand content from the

`

POLARIS data set. The performance of the model at the calibrations site is shown in Figure 10, and the performance for the validation sites is shown in Figure 11.

The performance of the general upscaling model was not as good as that of the site-specific models, but it was substantially better than using the point-scale data directly to represent the field-scale average without upscaling (Table 1). The NSE values for the general model ranged from a minimum of 0.855 for site A to a maximum of 0.972 at site C (Table 1). The NSE and RMSE values were improved or maintained with the general upscaling model versus without upscaling for all sites except site B. Site C showed the most dramatic improvement, 0.972 NSE with upscaling versus 0.057 NSE without. The large change in the NSE at site C was probably attributable to its high sand content. Site C RMSE values were also noticeably improved to 0.017 $cm^3\ cm^{-3}$ with upscaling versus 0.100 $cm^3\ cm^{-3}$ without upscaling.

The general upscaling model performed well at the validation sites with site 6 achieving the largest improvements in both NSE and RMSE after upscaling, 0.912 and 0.021 $cm^3\ cm^{-3}$ versus 0.428 and 0.055 $cm^3\ cm^{-3}$ without upscaling (Table 1). The NSE and RMSE values were identical, for site 5 with or without upscaling.

`

CHAPTER IV

DISCUSSION

This study used independent point-scale and field-scale soil moisture data sets to develop a general upscaling model that achieved RMSE values < 0.04 cm^3 cm^{-3} for each of six in situ monitoring stations. This level of accuracy meets the Soil Moisture Active Passive (SMAP) mission requirements of 0.04 cm^3 cm^{-3} (Entekhabi et al., 2010) and compares favorably with the accuracy obtained by site specific upscaling approaches in prior studies. The cosmic ray neutron rover enabled us to calibrate and validate a general upscaling model for point-scale in situ soil moisture sensors without the costs of installing enough sensors to effectively capture the areal average at the field-scale. Crow et al. (2012) summarized the number of point-scale soil moisture sampling sites necessary to characterize the field-scale mean (~800^2 m^2) with up to 12 sites required for an accuracy of 0.025 cm^3 cm^{-3} (Hupet and Vanclooster, 2002) and up to 35 sites for an accuracy of 0.02 cm^3 cm^{-3} (Brocca et al., 2007).

This study has shown comparable accuracy with other multi-scaling studies of similar scale. One such multi-site study in Africa achieved an NSE = 0.66 using data from two years at a study site (~25^2 km^2) with five sensor stations to estimate soil moisture at 1 km^2 (de Rosnay et al., 2009). In comparison, all of the site-specific NSE values were > 0.96 for the general upscaling model. Additionally, almost all of the soil moisture measurements were relatively low (< 10%), compared with the general upscaling model (0.067 to 0.45 cm^3 cm^{-3}).

`

Some limitations of this study are worth noting. The upscaling model is general in that it required no site-specific information beyond measured soil texture at the location of the in situ monitoring site, and it is general in the sense that it performs acceptably for each of four calibration sites and two validations sites. But these sites are all in the same field, and the applicability of this model to other sites is still unknown. Furthermore, validation site 5, is in close proximity (~25 m) to Site B, and all the point-scale monitoring locations are on topographic high points and do not fully capture the true heterogeneity of elevation across the study site. Likewise, the in situ monitoring locations do not represent the full range of NDVI observed across the site.

Finally, any biases in the point-scale or field-scale soil moisture data sets could impact the validity of the general upscaling model developed here. Such biases could arise from errors in the corrections or calibration applied to the cosmic-ray neutron data or in the calibration of the point-scale sensors.

`

CHAPTER V

CONCLUSION

The cosmic ray neutron rover, with measurements collected during 12 surveys over a period of twelve months, enabled the development of a general upscaling model which was able to successfully upscale point-scale soil moisture measurements from each of six monitoring sites within an 800^2 m^2 region at the MOISST site. As most upscaling studies focus on sites with multiple sensors or a network of sensors, this study has shown that accurate soil moisture estimates are achievable at the field-scale without the expense and maintenance of multiple moisture probes that are densely populated.

Future tests of the model should include data sets from different types of soil moisture sensors as well as different locations with varying soil textures, topography, and vegetation. This study has shown first steps toward a general upscaling approach that could be applied to any, and every, soil moisture monitoring station in the contiguous U.S. that has measured soil texture data. Such upscaling is needed to enhance the potential of existing in situ monitoring networks for meeting the soil moisture information needs for a wide array of land and water management decisions.

`

REFERENCES

Andreasen, M., Jensen, K. H., Desilets, D., Franz, T. E., Zreda, M., Bogena, H. R., andLooms, M. C. (2017). Status and Perspectives on the Cosmic-Ray Neutron Method for Soil Moisture Estimation and Other Environmental Science Applications. *Vadose Zone Journal, 16*(8). doi:10.2136/vzj2017.04.0086

Brocca, L., Morbidelli, R., Melone, F., andMoramarco, T. (2007). Soil moisture spatial variability in experimental areas of central Italy. *Journal of Hydrology, 333*(2-4), 356-373. doi:10.1016/j.jhydrol.2006.09.004

Chaney, N. W., Wood, E. F., McBratney, A. B., Hempel, J. W., Nauman, T. W., Brungard, C. W., andOdgers, N. P. (2016). POLARIS: A 30-meter probabilistic soil series map of the contiguous United States. *Geoderma, 274*, 54-67. doi:10.1016/j.geoderma.2016.03.025

Clewley, D., Whitcomb, J. B., Ruzbeh, A., Silva, A. R., Berg, A., Adams, J. R., . . . Moghaddam, M. (2017). A Method for Upscaling In Situ Soil Moisture Measurements to Satellite Footprint Scale Using Random Forests. *IEEE Journal of Selected Topics in Applied Earth Observations and Remote Sensing, Vol. 10, No. 6, June 2017, 10*(6).

Cosh, M. H., Jackson, T. J., Starks, P., andHeathman, G. (2006). Temporal stability of surface soil moisture in the Little Washita River watershed and its applications in

satellite soil moisture product validation. *Journal of Hydrology, 323*(1-4), 168-177. doi:10.1016/j.jhydrol.2005.08.020

Cosh, M. H., Ochsner, T. E., McKee, L., Dong, J., Basara, J. B., Evett, S. R., . . . Sayde, C. (2016). The Soil Moisture Active Passive Marena, Oklahoma, In Situ Sensor Testbed (SMAP-MOISST): Testbed Design and Evaluation of In Situ Sensors. *Vadose Zone Journal, 15*(4). doi:10.2136/vzj2015.09.0122

Crow, W. T., Berg, A. A., Cosh, M. H., Loew, A., Mohanty, B. P., Panciera, R., . . . Walker, J. P. (2012). Upscaling sparse ground-based soil moisture observations for the validation of coarse-resolution satellite soil moisture products. *Reviews of Geophysics, 50*(2). doi:10.1029/2011rg000372

De Lannoy, G. J. M., Houser, P. R., Verhoest, N. E. C., Pauwels, V. R. N., andGish, T. J. (2007). Upscaling of point soil moisture measurements to field averages at the OPE3 test site. *Journal of Hydrology, 343*(1-2), 1-11. doi:10.1016/j.jhydrol.2007.06.004

de Rosnay, P., Gruhier, C., Timouk, F., Baup, F., Mougin, E., Hiernaux, P., . . . LeDantec, V. (2009). Multi-scale soil moisture measurements at the Gourma meso-scale site in Mali. *Journal of Hydrology, 375*(1-2), 241-252. doi:10.1016/j.jhydrol.2009.01.015

Desilets, D., Zreda, M., andFerré, T. P. A. (2010). Nature's neutron probe: Land surface hydrology at an elusive scale with cosmic rays. *Water Resources Research, 46*(11). doi:10.1029/2009wr008726

`

Dong, J., andOchsner, T. E. (2018). Soil Texture Often Exerts a Stronger Influence Than Precipitation on Mesoscale Soil Moisture Patterns. *Water Resources Research, 54*(3), 2199-2211. doi:10.1002/2017wr021692

Dong, J., Ochsner, T. E., Zreda, M., Cosh, M. H., andZou, C. B. (2014). Calibration and Validation of the COSMOS Rover for Surface Soil Moisture Measurement. *Vadose Zone Journal, 13*(4). doi:10.2136/vzj2013.08.0148

Entekhabi, D., Njoku, E. G., O'Neill, P. E., Kellogg, K. H., Crow, W. T., Edelstein, W. N., . . . Van Zyl, J. (2010). The Soil Moisture Active Passive (SMAP) Mission. *Proceedings of the IEEE, 98*(5), 704-716. doi:10.1109/jproc.2010.2043918

Hess, W. N., Patterson, H. W., Wallace, R., andChupp, E. L. (1959). Cosmic-Ray Neutron Energy Spectrum. *Physical Review, 116*(2), 445-457. doi:10.1103/PhysRev.116.445

Hupet, F., andVanclooster, M. (2002). Intraseasonal dynamics of soil moisture variability within a small agricultural maize cropped field. *Journal of Hydrology*(261), 86-101.

Köhli, M., Schrön, M., Zreda, M., Schmidt, U., Dietrich, P., andZacharias, S. (2015). Footprint characteristics revised for field-scale soil moisture monitoring with cosmic-ray neutrons. *Water Resources Research, 51*(7), 5772-5790. doi:10.1002/2015wr017169

`

Loew, A., andSchlenz, F. (2011). A dynamic approach for evaluating coarse scale satellite soil moisture products. *Hydrology and Earth System Sciences, 15*(1), 75-90. doi:10.5194/hess-15-75-2011

McPherson, R. A., Fiebrich, C. A., Crawford, K. C., Kilby, J. R., Grimsley, D. L., Martinez, J. E., . . . Sutherland, A. J. (2007). Statewide Monitoring of the Mesoscale Environment: A Technical Update on the Oklahoma Mesonet. *Journal of Atmospheric and Oceanic Technology, 24*(3), 301-321. doi:10.1175/jtech1976.1

Ochsner, T. E., Linde, E., Haffner, M., andDong, J. (2019). Mesoscale Soil Moisture Patterns Revealed Using a Sparse In Situ Network and Regression Kriging. doi:10.1029/2018WR024535

Ott, L., andLongnecker, M. (2000). <*Statistical Methods and Data Analysis 5Ed.pdf*>: Duxbury Press.

Ritter, A., andMuñoz-Carpena, R. (2013). Performance evaluation of hydrological models: Statistical significance for reducing subjectivity in goodness-of-fit assessments. *Journal of Hydrology, 480*, 33-45. doi:10.1016/j.jhydrol.2012.12.004

Robinson, D. A., Campbell, C. S., Hopmans, J. W., Hornbuckle, B. K., Jones, S. B., Knight, R., . . . Wendroth, O. (2008). Soil Moisture Measurement for Ecological and Hydrological Watershed-Scale Observatories: A Review. *Vadose Zone Journal, 7*(1), 358-389. doi:10.2136/vzj2007.0143

`

Rosolem, R., Shuttleworth, W. J., Zreda, M., Franz, T. E., Zeng, X., andKurc, S. A. (2013). The Effect of Atmospheric Water Vapor on Neutron Count in the Cosmic-Ray Soil Moisture Observing System. *Journal of Hydrometeorology, 14*(5), 1659-1671. doi:10.1175/jhm-d-12-0120.1

Sharma, S., Carlson, J. D., Krueger, E. S., Engle, D. M., Twidwell, D., Fuhlendorf, S. D., . . . Ochsner, T. E. (2021). Soil moisture as an indicator of growing-season herbaceous fuel moisture and curing rate in grasslands. *International Journal of Wildland Fire, 30*(1). doi:10.1071/wf19193

Topp, G. C., Davis, J. L., andAnnan, A. P. (1980). Electromagnetic Determination of Soil Water Content: Measurements in Coaxial Transmission Lines. *Water Resources Research, 16*(No. 3), 574-582.

Western, A. W., Grayson, R. B., andBlöschl, G. (2002). Scaling of Soil Moisture: A Hydrologic Perspective. *Annual Review of Earth and Planetary Sciences, 30*(1), 149-180. doi:10.1146/annurev.earth.30.091201.140434

Whitcomb, J., Clewley, D., Colliander, A., Cosh, M. H., Powers, J., Friesen, M., . . . Moghaddam, M. (2020). Evaluation of SMAP Core Validation Site Representativeness Errors Using Dense Networks of In Situ Sensors and Random Forests. *IEEE Journal of Selected Topics in Applied Earth Observations and Remote Sensing, 13*, 6457-6472. doi:10.1109/jstars.2020.3033591

`

Zreda, M., Desilets, D., Ferré, T. P. A., andScott, R. L. (2008). Measuring soil moisture content non-invasively at intermediate spatial scale using cosmic-ray neutrons. *Geophysical Research Letters, 35*(21). doi:10.1029/2008gl035655

Zreda, M., Shuttleworth, W. J., Zeng, X., Zweck, C., Desilets, D., Franz, T., andRosolem, R. (2012). COSMOS: the COsmic-ray Soil Moisture Observing System. *Hydrology and Earth System Sciences, 16*(11), 4079-4099. doi:10.5194/hess-16-4079-2012

`

Table 1. Statistical comparison of field-scale average volumetric water content versus point-scale measurements at four calibration sites and two validation sites in the Marena, Oklahoma, In Situ Sensor Testbed (MOISST) without upscaling, after application of site-specific linear upscaling relationships, and after application of a general upscaling model. Statistical indicators include the Nash-Sutcliffe Efficiency (NSE), root mean squared error (RMSE), bias, regression slope, and regression intercept.

Site		Without upscaling			Site-specific linear upscaling					General upscaling		
		NSE	RMSE	Bias	Slope	Intercept	NSE	RMSE	Bias	NSE	RMSE	Bias
			$cm^3\ cm^{-3}$	$cm^3\ cm^{-3}$		$cm^3\ cm^{-3}$		$cm^3\ cm^{-3}$	$cm^3\ cm^{-3}$		$cm^3\ cm^{-3}$	$cm^3\ cm^{-3}$
Calibration Sites	A	0.772	0.047	-0.041	1.147	0.010	0.960	0.022	0.000	0.855	0.038	-0.030
	B	0.963	0.020	0.011	0.902	0.016	0.986	0.014	0.000	0.898	0.033	0.028
	C	0.057	0.100	-0.099	1.101	0.081	0.981	0.016	0.000	0.972	0.017	-0.003
	D	0.941	0.024	-0.012	1.194	-0.035	0.981	0.015	0.000	0.947	0.023	0.009
Validation Sites	5	0.951	0.015	-0.003	0.854	0.035	0.981	0.011	0.000	0.951	0.015	-0.002
	6	0.428	0.055	-0.051	1.322	-0.006	0.988	0.014	0.000	0.912	0.021	-0.010

`

Table 2. Depth-weighted sand content and clay content measured at four sites used to calibrate the general upscaling model and two sites used to validate the model. Also listed are elevation for each site determined using LIDAR data with 2-m resolution and average NDVI for the study period using 30-m resolution data from Landsat 8. The depth-weighted field average sand content and clay content from the POLARIS data set and field average elevation and NDVI are also listed.

	Site	Sand	Clay	Elevation (asl)	NDVI
		(%)	(%)	m	
Calibration sites	A	33.2	30.1	330	0.39
	B	34.9	28.1	329	0.42
	C	58.2	14.4	328	0.40
	D	35.8	26.7	332	0.40
Validation sites	Site 5	30.1	25.9	329	0.37
	Site 6	42.2	26.6	319	0.41
Field average		47.5	20.5	323	0.39

`

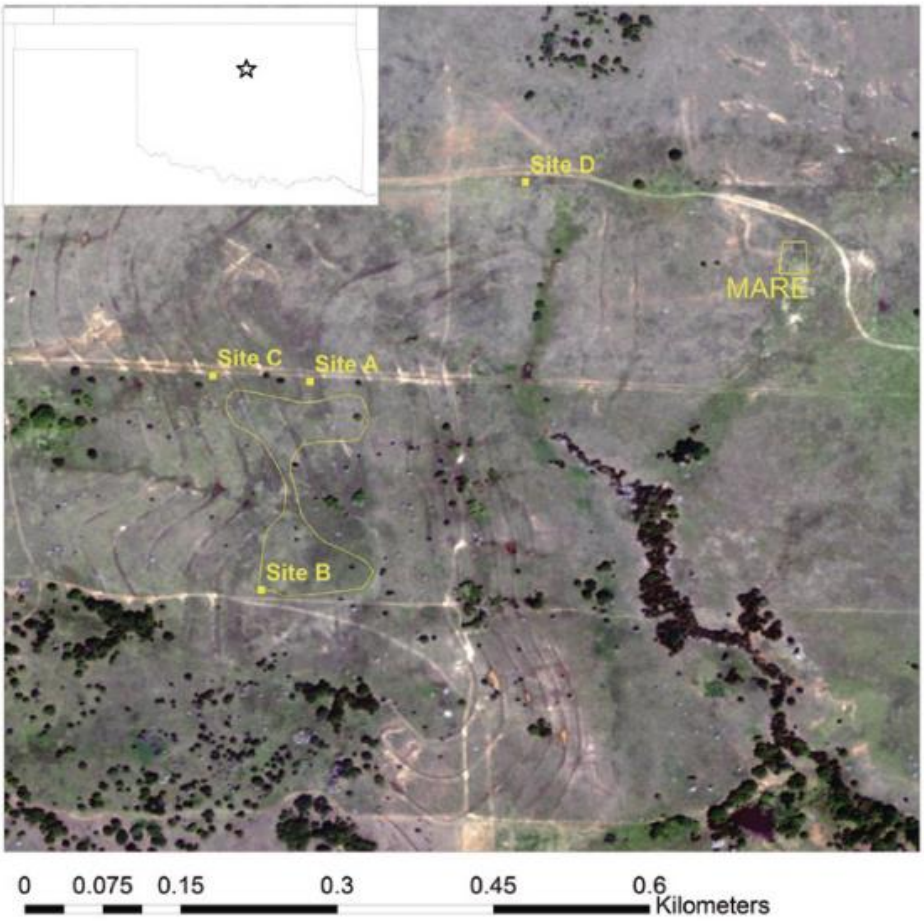

Figure 1. Map of the Marena, Oklahoma, In Situ Sensor Testbed (MOISST), located southwest of Stillwater, OK. Yellow letters designate in situ monitoring sites (A-D) and the upper right quadrant shows the Oklahoma Mesonet site (MARE). Reproduced from Cosh et al. (2016).

`

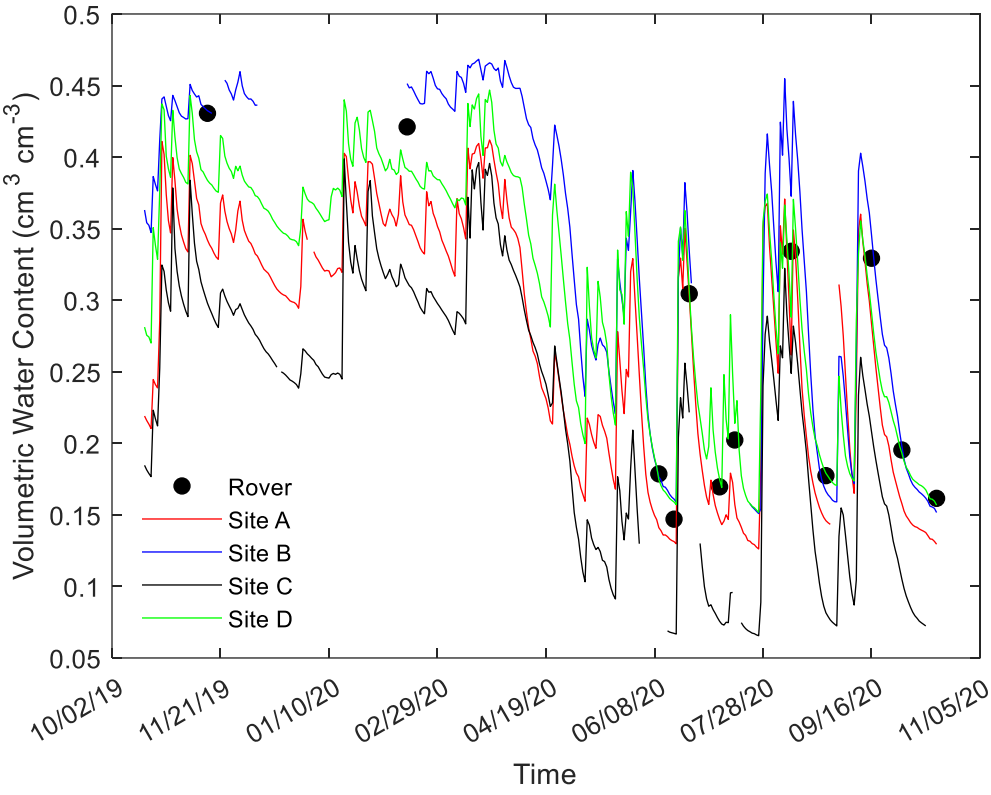

Figure 2. Depth-weighted volumetric water content data from four in situ monitoring sites during the period of the study. Black circles are field-scale averages measured using the rover on each survey date.

`

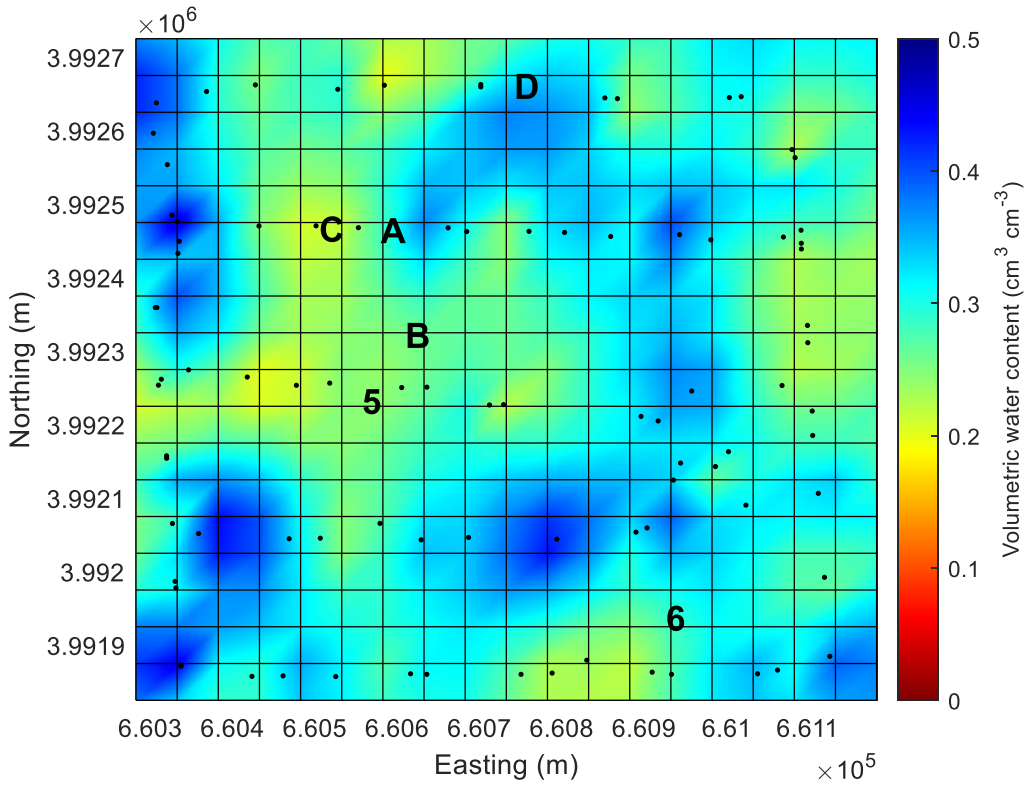

Figure 3. Map displaying kriged soil volumetric water content estimates derived from the rover data on 16 Sep. 2020, averaging 0.329 cm^3 cm^{-3}. Black dots represent the locations of rover measurements. Coordinates are UTM, Zone 14.

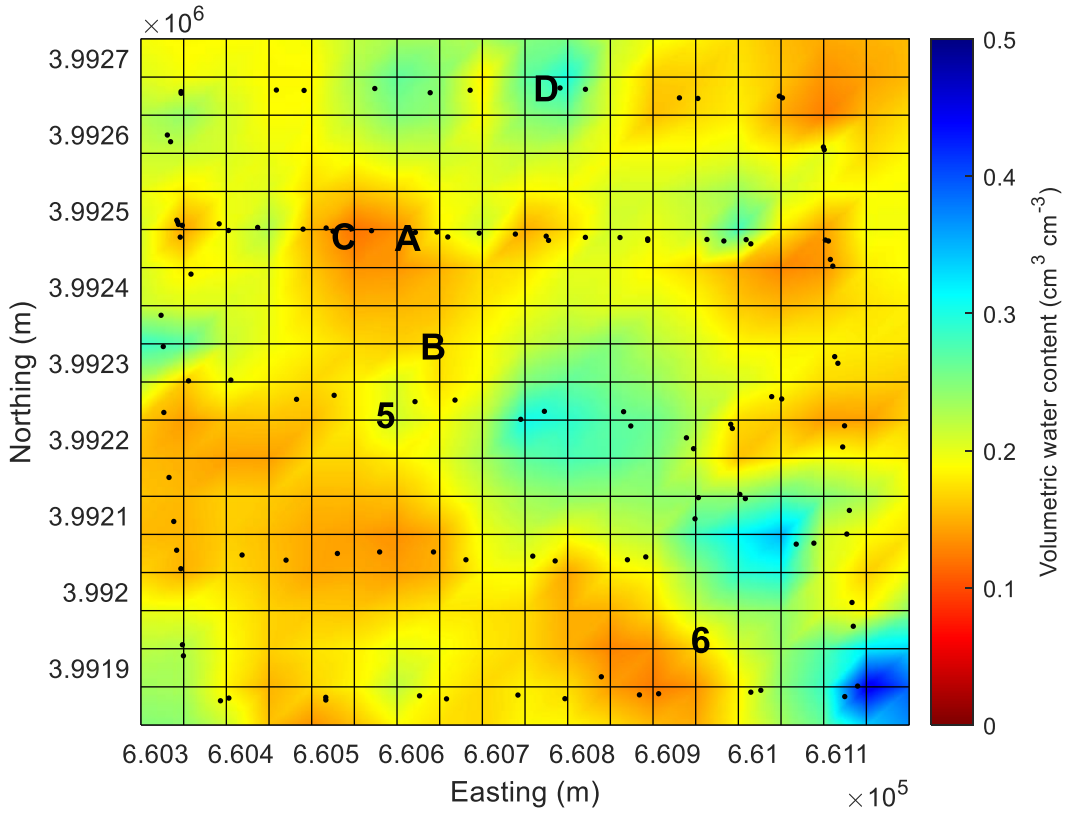

Figure 4. Map displaying kriged soil volumetric water content estimates derived from the rover data on 30 Sep. 2020, averaging 0.195 cm^3 cm^{-3}. Black dots represent the locations of rover measurements. Coordinates are UTM, Zone 14.

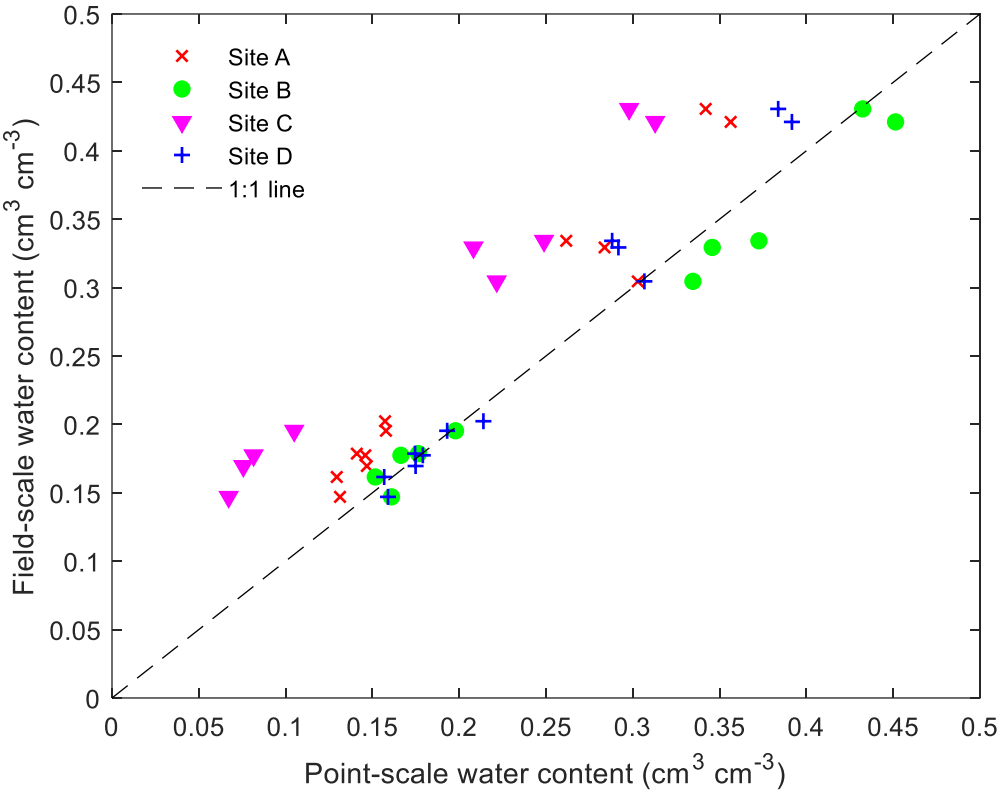

Figure 5. Comparison of field-scale volumetric water content estimate from the cosmic-ray neutron rover surveys vs. depth-weighted point-scale volumetric water content measurements from the in situ sensors at four sites for the twelve survey dates. Days with missing point-scale data from particular sites were omitted.

`

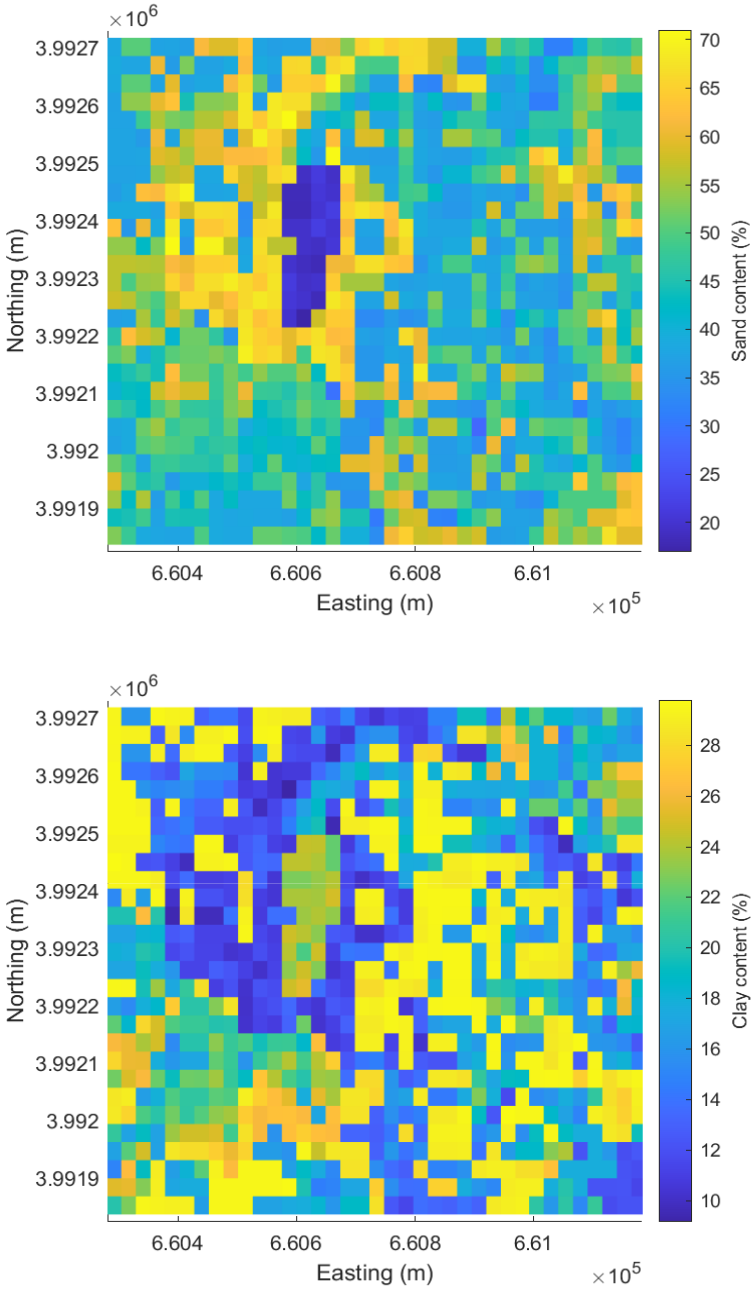

Figure 6. Depth-weighted sand content (top) and depth-weighted clay content (bottom) for the study site based on 30-m resolution POLARIS data. Coordinates are UTM, Zone 14.

`

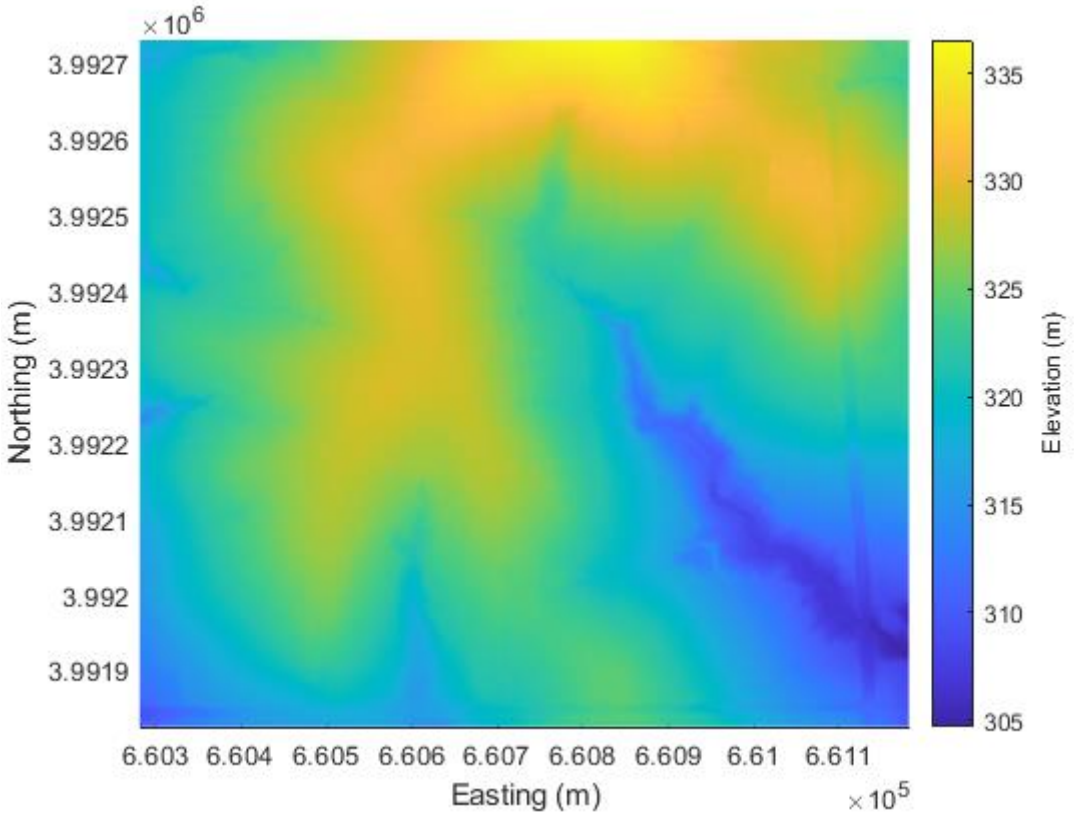

Figure 7. Map of elevation at the study site based on 2-m horizontal resolution LIDAR data from USGS. Coordinates are UTM, Zone 14.

`

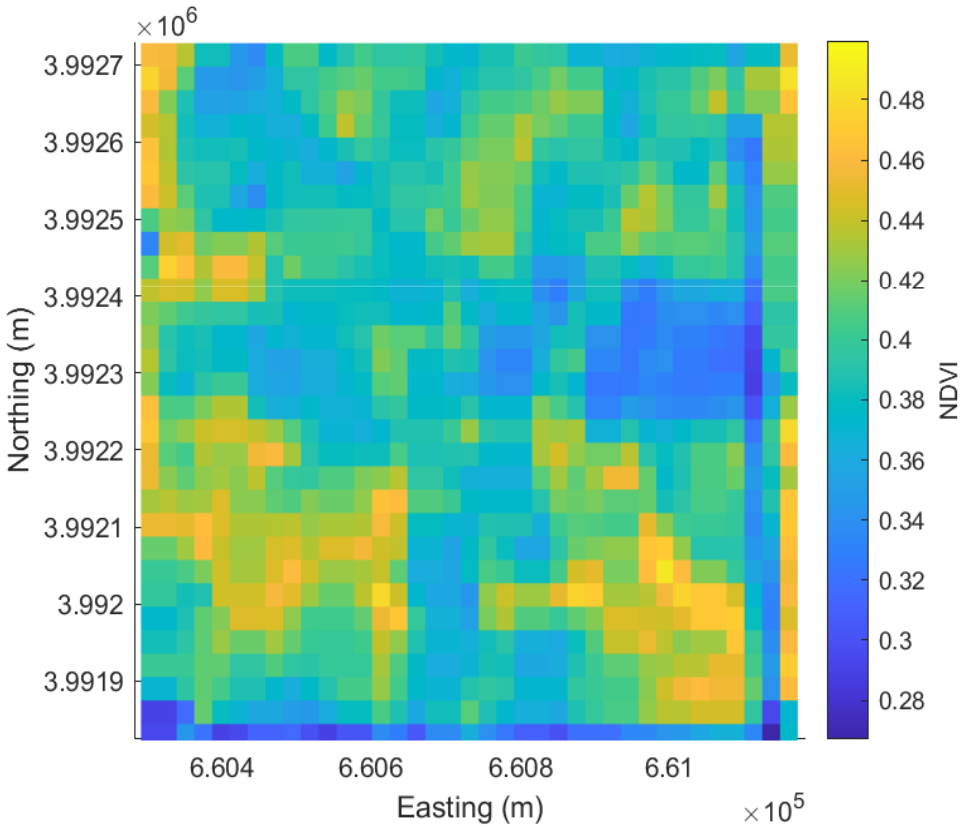

Figure 8. NDVI for the study site averaged over the period of Nov. 2019 – Oct. 2020 based on 30-m resolution Landsat 8 data. Coordinates are UTM, Zone 14.

`

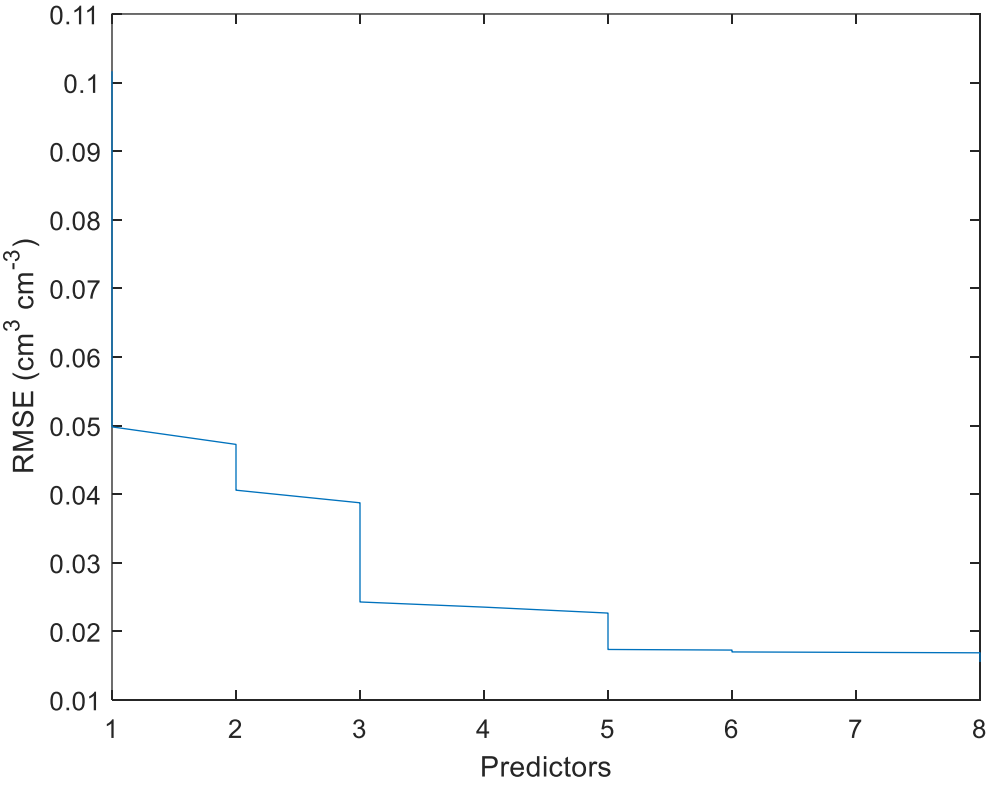

Figure 9. LASSO regression results showing number of predictor variables used and estimated RMSE. The most influential predictor variables were: (1) point-scale volumetric water content , (2) sand content, and (3) NDVI.

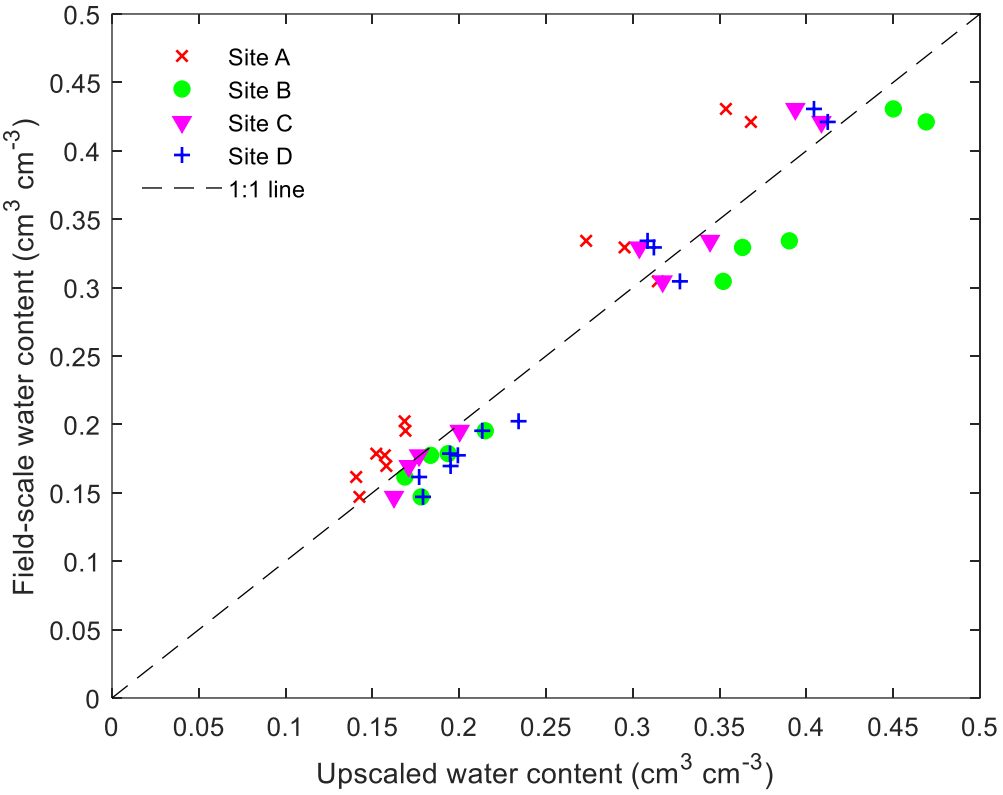

Figure 10. Upscaled soil volumetric water content estimates from each of the four calibration sites after applying the general upscaling model compared with the field-scale water content measurements from the cosmic-ray neutron rover.

`

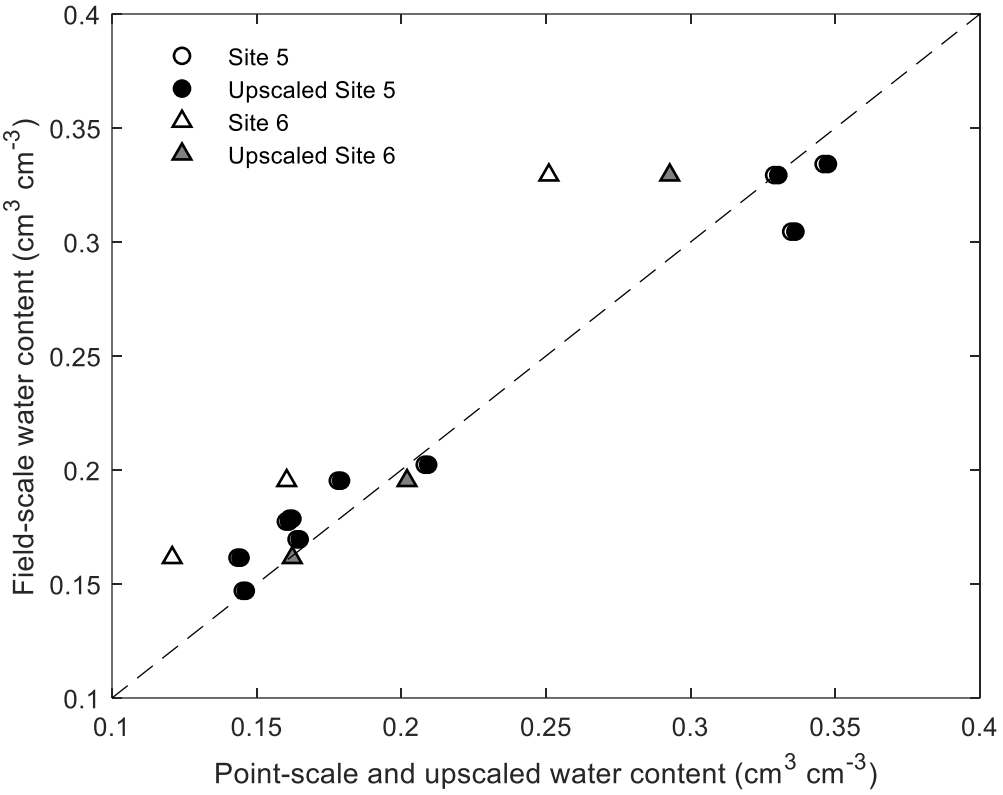

Figure 11. Point-scale soil volumetric water content measurements from each of the two validation sites and upscaled water content estimates for those sites after applying the general upscaling model compared with the field-scale water content measurements from the cosmic-ray neutron rover.

`

APPENDICES

Table A1. Soil physical properties for calibration sites A, B, C, and D.

	Depth (cm)		Particle size distribution		
Site	Midpoint	Bulk Density	% Sand	% Silt	% Clay
A	2.5	1.29			
A	7.5	1.40	34	38	28
A	15	1.60	28	34	37
A	25	1.51	48	24	28
A	35	1.73	26	41	33
A	45	1.72	31	31	38
A	55	1.72	23	34	42
A	65	1.81	21	41	38
A	75	1.77	24	46	30
B	2.5	1.38			
B	7.5	1.42	38	39	23
B	15	1.49	26	31	43
B	25	1.44	13	28	59
B	35	1.52	14	32	54
B	45	1.64	5	37	58
B	55	1.61	0	44	56
B	65	1.71	2	41	58
B	75	1.75	0	47	53
C	2.5	1.06			
C	7.5	1.52	59	28	13
C	15	1.46	57	27	16
C	25	1.40	49	27	24
C	35	1.53	49	25	25
C	45	1.55	70	16	14
D	2.5	0.99			
D	7.5	1.39	37	38	24
D	15	1.45	33	35	32
D	25	1.51	25	34	41
D	35	1.59	19	34	48
D	45	1.69	25	31	44
D	55	1.66	20	34	47
D	65	1.65	24	32	44
D	75	1.75	30	28	41
D	85	1.79	30	28	41
D	95	1.81	30	30	40

`

Table 2. Soil physical properties for validation sites, JFSP sites 5 and 6.

	Depth (cm)		Particle size distribution		
Site	Midpoint	Bulk Density	% Sand	% Silt	% Clay
5	5	1.37	30	19.7	50.2
5	10	1.37	32.2	32	35.8
5	20	1.42	23.4	48	28.6
5	50	1.59	18.7	43.9	37.4
6	5	1.19	43.4	23.5	33.1
6	10	1.41	43.3	27.4	29.3
6	20	1.32	32.8	41	26.2
6	50	1.57	9.9	59.8	30.2

`

VITA

William Gerald Brown Jr.

Candidate for the Degree of

Master of Science

Thesis: UPSCALING SOIL MOISTURE MEASUREMENTS FROM IN SITU SENSORS

Major Field: Plant and Soil Sciences

Biographical:

Education:

Completed the requirements for the Master of Science in Plant and Soil Sciences at Oklahoma State University, Stillwater, Oklahoma in July 2021.

Completed the requirements for the Bachelor of Science in Environmental Science at Oklahoma State University, Stillwater, Oklahoma in May 2019.

Experience: Graduate Research Assistant, Soil Physics Lab

Professional Memberships: Soil Science Society of America